Available online at www.sciencedirect.com
ScienceDirect
Biochemical and Biophysical Research Communications 367 (2008) 26–32
BBRC
www.elsevier.com/locate/ybbrc

Molecular modelling of miraculin: Structural analyses and functional hypotheses

Antonella Paladino [a,b,c], Susan Costantini [a,b,c], Giovanni Colonna [b,c], Angelo M. Facchiano [a,b,*]

[a] *Laboratory of Bioinformatics and Computational Biology, National Council of Researches, Institute of Food Sciences ISA – CNR, via Roma 52A/C, 83100 Avellino, Italy*
[b] *CRISCEB – Second University of Naples, via Costantinopoli 16, 80138 Napoli, Italy*
[c] *Department of Biochemistry and Biophysics – Second University of Naples, via Costantinopoli 16, 80138 Napoli, Italy*

Received 6 December 2007
Available online 26 December 2007

Abstract

Miraculin is a plant protein that displays the peculiar property of modifying taste by swiching sour into a sweet taste. Its monomer is flavourless at all pH as well as at high concentration; the dimer form elicits its taste-modifying activity at acidic pH; a tetrameric form is also reported as active. Two histidine residues, located in exposed regions, are the main responsible of miraculin activity, as demonstrated by mutagenesis studies. Since structural data of miraculin are not available, we have predicted its three-dimensional structure and simulated both its dimer and tetramer forms by comparative modelling and molecular docking techniques. Finally, molecular dynamics simulations at different pH conditions have indicated that at acidic pH the dimer assumes a widely open conformation, in agreement with the hypotheses coming from other studies.

Keywords: Miraculin; Sweet proteins; Molecular modelling; Molecular dynamics; Protein assembly

Six sweet tasting proteins, ranging in size from 6 to ~22 kDa, have been discovered [1]: miraculin in 1968 [2], thaumatin and monellin in 1972 [3,4], curculin in 1990 [5], mabinlin in 1993 [6], and brazzein in 1994 [7]. All six proteins, extracted from fruits of tropical plants, display activity as sweeteners or taste-modifiers. In the last 30 years many efforts have been made to commercially exploit the use of sweet-tasting proteins. In order to understand the molecular bases that induce the sweetness of thaumatin, monellin, brazzein, and neoculin, some structural studies were made and some residues were identified as potential responsible for their sweetness [8].

Miraculin has been isolated from the fruit of Richadella Dulcifica in West Africa, and although it does not show the intrinsic ability of inducing sweetness, it is able of switching sour into a sweet taste. Miraculin is a single polypeptide chain having molecular weight of 24,600 kDa and two sugars linked to two Asn residues [9]. The pure form and that denatured of the miraculin are constituted of a tetramer and a dimer, respectively. Both tetramer and dimer miraculin in crude state have the taste-modifying activity [10]. Miraculin dimer, covalently linked by an inter-chain disulphide bond, shows its taste-modifying activity at acidic pH, with maximum at pH 3.0, and is flat at neutral pH and almost inactive at pH 6.0. Monomeric miraculin, even at high concentrations, is flavourless at all pHs and its dimerization is required in order to trigger its activity. As it has been suggested, this pH-sweetness relationship could be reminiscent of the imidazole titration curve. Mutagenesis studies indicated the two His residues (i.e. His29 and

* Corresponding author. Address: Laboratory of Bioinformatics and Computational Biology, National Council of Researches, Institute of Food Sciences – CNR, via Roma 52A/C, 83100 Avellino, Italy. Fax: +39 0 825781585.
E-mail address: angelo.facchiano@isa.cnr.it (A.M. Facchiano).

0006-291X/$ - see front matter © 2007 Elsevier Inc. All rights reserved.
doi:10.1016/j.bbrc.2007.12.102

His59) as the main responsible of the taste-modifying activity [11].

Previous studies showed that sweet proteins elicit their function through the binding to T1R2 – T1R3 heterodimer, a G-protein coupled receptor which binds also natural sugars and artificial sweeteners. The evident differences between the mass of these proteins and small sweeteners molecules suggest that different binding sites should exist on the receptor surface. Studies aimed to identify these binding sites could clarify the molecular events leading to receptor activation [12]. Recent studies suggested also that the association of the closed and open forms of monomers constituting the T1R2 – T1R3 hetero-dimer can create a large charged cavity where sweet proteins fit exerting their function [13–17].

No atomic level structural data are available for miraculin. We simulated the three-dimensional structure of glycosylated miraculin, its dimer and tetramer forms by comparative modelling and molecular docking strategy. Moreover, in order to analyse the stability of miraculin dimer, we conducted molecular dynamics simulations at acidic and neutral pH.

Methods

Molecular modelling. The sequence of miraculin from Richadella dulcifica [9] was analysed with BLAST [18] to find similar proteins in databases. The three-dimensional model of miraculin region 31–220 was created by comparative modelling, according to the procedure already used and described in details in our previous works [19–22], using the template model of a homologous Kunitz (STI) type inhibitor [PDB code: 1R8N] from seeds of Delonix Regia [23]. Protein sequences were aligned with CLUSTALW [24]. MODELLERv7 [25] implemented in InsightII (Accelrys, San Diego, CA) was used to build 10 full-atoms models. The best model was selected using PROCHECK [26] to evaluate the stereochemical quality of the models and their structural packing quality, and ProsaII [27] to check the fitness of sequence to structure and to assign a scoring function. All models were analysed also by other validation programs, i.e., Anolea [28], Victor/FRST [29] and Profiles3D (InsightII, Accelrys, San Diego, CA). In the selected model the loop regions were refined using the LOOPY module of Jackal package [30]. LOOPY appeared to yield the best results for loop modelling, with models that are on average of 2–8% better than those generated by other programs [31]. In details, the LOOPY module generates a large number of random conformations via ab-initio method, minimizing each of the random candidates and selecting the best candidates using colony energy, and fuses loop in order to sample more conformation space, repeating the process until convergence. Cysteine side-chains refinement was performed by SCAP module of Jackal package [30]. Secondary structures were assigned by the DSSP program [32]. A search for structural classification was performed on CATH database [33]. Secondary structure predictions were performed with Jpred [34] and PHD [35] servers. Molecular superimposition, RMSD values and figures were obtained with the InsightII package (Accelrys, San Diego, CA).

The carbohydrate chains were built using the Biopolymer module in InsightII (Accelrys, San Diego, CA). Hydrogen atoms were added with the "Modify/Add Hydrogens tool". These structures were optimized according to the optimization protocol of the Builder module in InsightII, starting with the steepest descent method and switching to the conjugate gradient algorithm only when the energy gradient reached the default threshold value.

Simulation of glycosylated miraculin monomer. To simulate the *N*-glycosylated miraculin structure, two identical sugars were bound to the modelled monomer chain, creating *N*-glycosydic bonds with Asn 41 and Asn 185 by using the Builder module of Insight II.

This sugar–protein system was minimized for 500 steps under conjugate gradient algorithm and then subjected to molecular dynamics simulations using Consistent Valence Force Field (CVFF) to assign potentials and charges and moving only the loop regions supporting the glycosylated residues. 300-ps long MD simulations were performed at 300 K with a time step of 1 fs, setting the dielectric constant to 1 and using the Discover module in InsightII. Conformations were saved every 1000 steps (i.e. every 1 ps). Data recorded during the last 100 ps were used for further analyses.

Modelling of miraculin dimer and tetramer. The homodimer of miraculin was simulated by creating SS-bond between the Cys137 of a monomer and the corresponding cysteine of another identical monomer with Builder module of Insight II. Attempts in dimer design were also made using the docking web server CLUSPRO [36] that resulted the best docking program in CAPRI 2005 experiment with a success rate of about 71% [37]. CLUSPRO is a fast algorithm for filtering docked conformations with good surface complementarity, and ranking them based on their clustering properties; the free energy filters select complexes with lowest desolvation and electrostatic energies [36]. ZDOCK implemented in CLUSPRO was selected to perform the initial rigid-body docking, where scoring function includes a combination of shape complementarity.

The dimer models were selected by considering the oligosaccharides volumes to avoid steric hindrance and by evaluating some features and parameters. The "Protein–Protein Interaction Server" [38] and NACCESS program [39] were used to identify the amino acids at the interface in the miraculin dimers and tetramers and to evaluate their solvent accessibility. The presence of putative H-bonds was calculated with "Hbond tool" in InsightII (Accelrys, Inc., San Diego, CA, USA) and Hbplus program [40].

The selected dimer was minimized by using 500 steps of energy minimization under conjugate gradient algorithm in order to optimize side chain conformations and avoid sterical clashes according to the commonly used procedure [20,21,41,42].

Miraculin tetramer models were simulated and analysed using the same procedure and programs as for dimer modelling.

Molecular dynamics simulations. MD simulations were performed with GROMACS software package (v3.3.1) [43]. Models were put in triclinic boxes full of SPC216 water molecules and GROMOS43a1 was selected as force-field. In order to optimize the system the models were previously subjected to energy minimization and position restraints cycles. The simulations were carried out with periodic boundary conditions and bond lengths were constrained by the LINCS algorithm. Part Mesh Ewald (PME) algorithm was used for the electrostatic interactions with a cut-off of 0.9 Å, according to recent paper [44].

Simulations were conducted at different pH values. At neutral pH, it is assumed that tritable groups of His, Glu and Asp residues are unprotonated while the acidic condition (pH ~3) is reached when all these groups are protonated. All simulations were run for 10 ns at room temperature (300 K) coupling the system to an external bath.

GROMACS and VMD routines [45] were utilized to check trajectories and the quality of the simulations.

The center of mass of monomers costituing each dimer and their distance has been calculated using a CGI script in Perl language developed in our group.

Results and discussion

Modelling of N-glycosylated miraculin monomer

Mature miraculin is a homodimer made by two chains which have two *N*-glycosylated Asn residues and are cross-linked through a disulphide bridge. Sequence similarity searches showed that miraculin has high sequence similarity ($E_{\text{value}} = 6e^{-13}$) to many members of the STI family of proteases inhibitors. We modelled the 3D struc-

ture of miraculin using the crystal structure of the homologous Kunitz (STI) type inhibitor (PDB code: 1R8N) from seeds of Delonix Regia because the sequence identity between these two proteins resulted of 33%. In Fig. 1 we show miraculin/template alignment. Four cysteines involved in two disulphide bridges in the template structure are aligned to four related cysteines in the miraculin sequence. Miraculin has three additional cysteines, two of which form another disulphide bond in the monomer, the third makes the interchain bridge. Starting from this refined alignment with the reference structure, a set of full-atoms models was generated. The best model (Fig. 2A) has 89.2% of residues in most favoured regions, Prosa Z-score of −5.81, Anolea Z-score of −535.390, Victor/FRST function value of −20731.029 and Profiles3D score of 57.34. These values, compared also with that of the template structure, indicate that a good quality model has been created. About 31% of the residues assumes a β-strand conformation, organized in six two-stranded hairpins. Three of these form a barrel structure and the other three are in a triangular array that caps the barrel. Secondary structure predictions made by JPRED and PHD programs agree with the obtained structure of miraculin by comparative modelling (see Fig. 1). Superposition of the modelled protein with the template structure gave RMSD value of 0.52 Å for secondary structure conserved regions, suggesting that our model keeps the typical β-trefoil architecture of Kunitz inhibitor family [33].

The miraculin model presents six cysteine residues involved in three disulphide bridges. These three intrachain disulphide bridges (Cys46-Cys91, Cys147-Cys158, and Cys151-Cys154) stabilize each monomer, in agreement to experimental data [11]. His29 and His59, indicated as key residues for the taste-modifying properties, are in loop regions and well exposed (see Table 1). The N-linked glycosylation sites (i.e. Asn41 and Asn185) are also in exposed loop regions. All together these features of our model are reliable with those expected by previous experimental evidences.

The carbohydrate chain [(Man)3 (GlcNAc)2 (Fru)1 (Xyl)1] (Fig. 2A) was attached to the Nδ2 of Asn41 and Asn185, as described in Methods [10,46,47].

Modelling of miraculin dimer

The miraculin dimer is shown in Fig. 2B. His29 is more exposed than His59 (see Table 1), according to the experimental data [11]. This finding hints that His29 could cover the major role in the miraculin taste-modifying activity. Therefore, we detected and analysed the charged regions around the His residues which could be suitable for the binding to the taste receptor and the elicitation of its taste-modifying activity. In particular, we noticed that many charged residues are in the proximity of His29 (Arg27, Asp28, Arg54, Glu56, Asp166, Arg171, Arg172, Asp177, Lys178, and Glu183). This observation would provide a good rationale for the electrostatic interactions occurring between the negatively charged cavity of the T1R2–T1R3 and the positive zone of the protein, as suggested [14,48,49]. A similar analysis for His59 found a smaller charged area (Arg54, Lys55, Glu56, Asp58, Asp60, Arg61, and Lys186).

In the selected dimer, carbohydrate moieties are localized at the edges of the dimeric protein, in exposed areas and they do not form important interactions with the protein body. Carbohydrate contents would not be involved in the taste-modifying activity, similarly to the other glycosylated sweet protein, neoculin [16].

```
1R8N       SDAEKVYDIEGYPVFLGSEYYIVSAIIGAGGGGVRPGRTRG--SMCPMSIIQEQSDLQMG    58
MIR        SAPNPVLDIDGEKLRTGTNYYIVPVLRDHGGGLTVSATTPNGTFVCPPRVVQTRKEVDHD    60
JPRED      -----EE-----------EEEEEEEE------EEEEE-----------EEEEE-------
PHD        -----EEE----EE----EEEEEEEE------EEEEEE----------EEEE--------
           * .: * **:*  :  *:.****..: . *** . .. * .   :**  ::* :.::: .

1R8N       LPVRFSSPEEKQGKIYTDTELEIEFVEKPDCAESSKWVIVKD-----SGEARVAIGGSED    113
MIR        RPLAFFPENPKEDVVRVSTDLNINFSAFMPCRWTSSTVWRLDKYDESTGQYFVTIGGVKG    120
JPRED      --EEEE-------EEEE--EEEEEE------------EEEEE-------EEEEEE-----
PHD        -EEEEEE------EEEE---EEEEEEE----------EEEEEE-------EEEEE-----
           *: * . : *:. : ..*:*:*:*      *  :*. *   *     :*:  *:*** :.

1R8N       HPQGELVRGFFKIEKLG-SLAYKLVFCP---KSDSGSCSDIGINYE--GRRSLVLKSSDD    167
MIR        NPGPETISSWFKIEEFCGSGFYKLVFCPTVCGSCKVKCGDVGIYIDQKGRRRLALS---D    177
JPRED      ---------EEEEEEE-----EEEEEE-------------EEEE-----EEEEE-----
PHD        ---------EEEEEEE----EEEEEEE------------EEEEEE-----EEEEEE----
           :*  * : .:****::  *  *******    * . .*.*:**  :  *** *.*.   *

1R8N       VPFRVVFVKPRSGSETES  189
MIR        KPFAFEFNKTVYF-----  190
JPRED      --EEEEEEE---------
PHD        --EEEEEEE---------
            ** . * *.
```

Fig. 1. CLUSTALW sequence alignment of Soybean Trypsin Inhibitor (PDB code = 1R8N) and Miraculin (UniProt Accession Number P13087). Asterisks (*) indicate conserved amino acids. Cys residues are in bold type. Glycosylated Asn residues are in grey. Amino acids in β strands are underlined. Amino acids in 3_{10} helix are in bold italic. JPRED and PHD are the secondary structure predictions and E indicate β-strands.

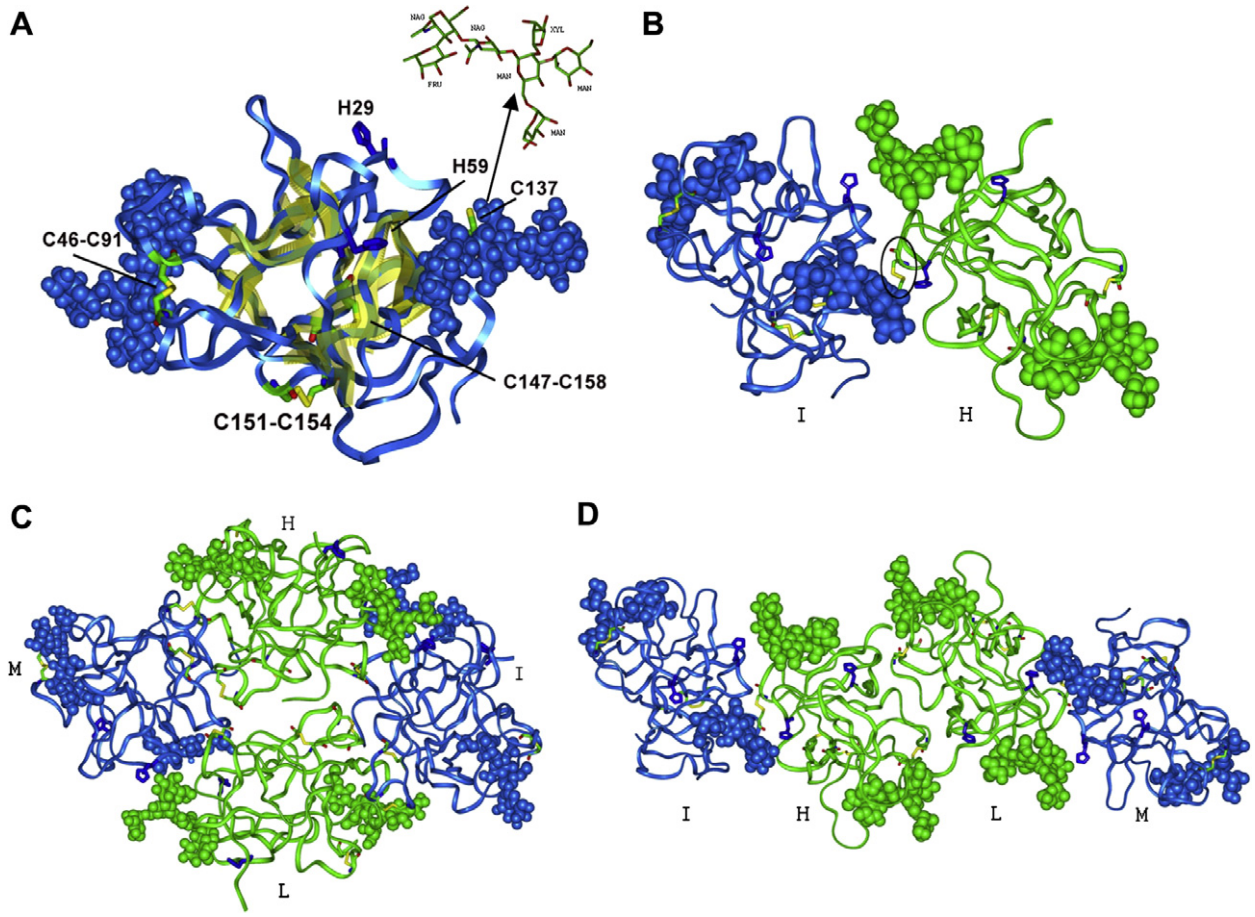

Fig. 2. 3D molecular model of Miraculin. Backbone ribbon is shown. Cys and His residues are indicated in stick and coloured by atom type and blue, respectively. Sugars are in CPK. (A) monomer form with detailed view of the glycidic chain shown in stick and coloured by atom type. The secondary structure topology is shown: yellow cartoons represent β-strands; (B) miraculin dimer. First and second monomer are coloured in green and blue and indicated as chain H and I, respectively. Oval indicates the inter-chain disulphide bond (C137–C137). (C and D) Globular and linear forms of miraculin tetramer, respectively. Identical colours are used for the corresponding monomers of two dimers (H and I; L and M) in the tetramers. (For interpretation of the references to colour in this figure legend, the reader is referred to the web version of this article.)

Table 1
Accessible surface area of His (H29, H59, H*29, and H*59, corresponding histidines of the two monomers of the dimer; h29, h59, h*29, and h*59, histidines of the second dimer forming the tetramer) expressed in $Å^2$ in the starting models

ASA	Dimer	Globular tetramer	Linear tetramer
H29	69.9	69.7	70.7
H59	53.0	53.0	52.9
H*29	72.3	72.8	73.1
H*59	50.3	51.0	51.1
h29		69.8	70.4
h59		54.5	52.6
h*29		72.0	72.0
h*59		50.6	49.9

Modelling of miraculin tetramer

The miraculin tetramers were obtained using the above mentioned CLUSPRO web server. Two different orientations of the dimers can be summarized, both compatible with the presence of the sugar chains. Dimers association leads to a globular and a linear tetrameric conformation (Fig. 2C and D). Both tetrameric models result structurally reliable and without discrepancies with the alone dimer features regarding histidines positions, their exposure and charged surfaces (Table 1). Sugar chains do not present any steric hindrance. In the globular model, four H-bonds are formed between the two dimers and 46 residues for each subunit are at the interface, while in the linear form only one H-bond is possible between the two dimers and almost half is the number of the residues at the interface. The globular and linear conformations may represent the "closed" and "open" forms of tetramer miraculin, respectively.

Molecular dynamics simulations of miraculin dimer

Previous works conducted on neoculin highlighted a macroscopic conformational change occurring in the global architecture of the molecule at acidic pH [16]. Neoculin may adopt a widely "open" conformation at acidic pH (~2.5), while unprotonated neoculin at neutral pH adopts a "closed" conformation. Moreover, the His residues of

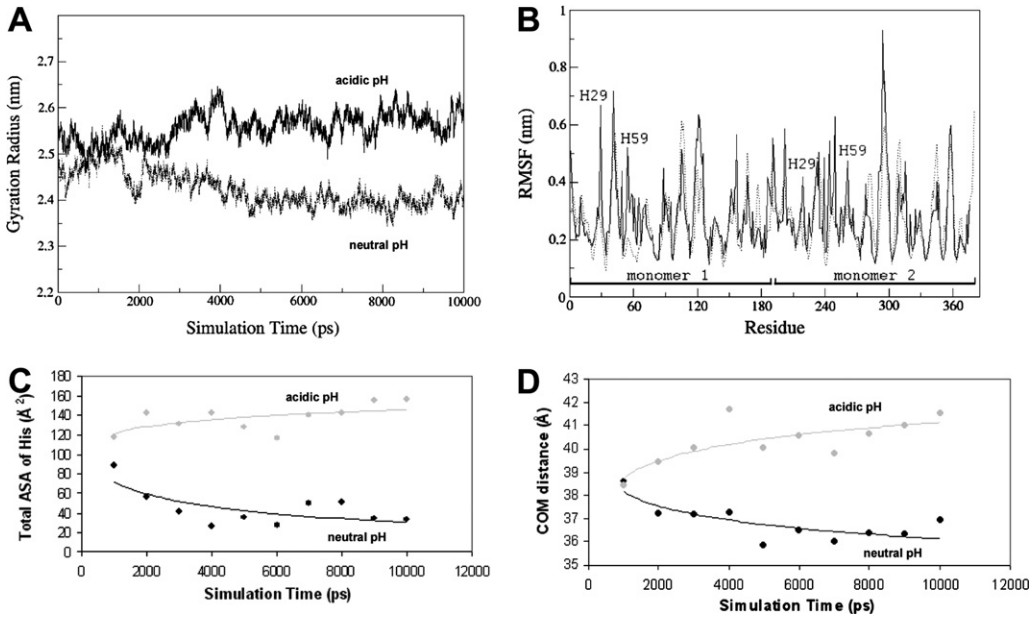

Fig. 3. MD simulations evolution conducted at acidic and neutral pH: (A) gyration radius; (B) root mean square fluctuations (RMSF) for the C-alpha atoms; dot-line: neutral pH, continuous line: acidic pH; (C) Accessible Surface Area of His calculated in the two simulations computed every 1000 ps; (D) Centers of mass distances in the two simulations computed every 1000 ps.

this molecule resulted to play a central role in the elicitation of its activity.

Thus, MD simulations were conducted on the dimeric miraculin, either at neutral pH or acidic pH. At acidic pH (~3.0), the completely protonated dimeric model reaches a stable equilibrated state after 4 ns simulation, even though it is worth noticing that the fluctuation observed in the first 3000 ps are more severe in comparison to the simulation executed at neutral pH. In the following time, protein looks very stable, as confirmed by all the indicators commonly used to analyse MD simulations (gyration radius, root mean square fluctuation, secondary structure evolution, and number of H-bonds, etc.) (Fig. 3A, 3B and 1S, 2S). The global architecture of the model is kept during the whole simulation, even if more flexible regions are also observed compared to neutral pH simulation as shown by H-bond plots (Fig. 1S) and secondary structure evolution (Fig. 2S).

In order to compare the dynamical properties of two systems at different pH, we computed the gyration radii (Fig. 3A). The gyration radius trends clearly display a different evolution: a decrease of the molecule compactness is registered at acidic pH, while miraculin seems to become more compact at neutral pH. We also report root mean square fluctuations of the two simulations (Fig. 3B) that mainly involve loop regions either at acidic or neutral pH. Further, at acidic pH, some extra flexible fragments are present in specific areas of the protein surface. Visibly, the superposition of the RMS fluctuations of the neutral and acidic simulations reveals that the additional regions having a high degree of flexibility fall in the proximity of the His residues.

Moreover we evaluated the solvent accessible surface area of the His residues (His29, His59). His accessibility (Fig. 3C) increases during the simulation at acidic pH with a correlation coefficient of 0.6. Notably this value decreases in the other simulation.

A measure of the opening of the two subunits of the dimer, which seem fixed in the dimeric association only by the inter-chain disulphide bond, according to Shimizu-Ibuka et al. [16], is reported in Fig. 3D in terms of center of mass distances along the trajectories. At acidic pH, the distance between the two monomers of the dimer increases, while at neutral pH the two subunits get closer. The structural rearrangement of the subunits decreases the distance between the His29 residues at acidic pH, so that their surrounding surfaces become closer and constitute an unique basic region on the dimer surface.

All these results agree with the hypothesis that sweet proteins exert their activity by the interaction of a basic surface with the negative cavity of the taste receptor [13,15]. Our model of miraculin structure gives the opportunity to make deeper investigations about the miraculin-receptor interaction.

Further studies are under development in our group to simulate the effect of His residues mutations and verify the role of these charged residues in the structural rearrangements observed during the simulations.

Acknowledgments

This work was partially supported by the CNR-Bioinformatics Project. Computations were performed on the cluster ‘‘LILLIGRID’’ at the Istituto per le Applicazioni del Calcolo ‘Mauro Picone’ – Naples. We also thank Luigi

Vitagliano and Luciana Esposito for useful suggestions on molecular dynamics studies.

Appendix A. Supplementary data

Supplementary data associated with this article can be found, in the online version, at doi:10.1016/j.bbrc.2007.12.102.

References

[1] I. Faus, Recent developments in the characterization and biotechnological production of sweet-tasting proteins, Appl. Microbiol. Biotechnol. 53 (2) (2000) 145–151.
[2] K. Kurihara, L.M. Beidler, Taste-modifying protein from miracle fruit, Science 161 (847) (1968) 1241–1243.
[3] H. Van der Wel, K. Loeve, Isolation and characterization of thaumatin I and II, the sweet-tasting proteins from Thaumatococcus daniellii Benth, Eur. J. Biochem. 31 (2) (1972) 221–225.
[4] J.A. Morris, R.H. Cagan, Purification of monellin, the sweet principle of Dioscoreophyllum cumminsii, Biochim. Biophys. Acta 261 (1) (1972) 114–122.
[5] H. Yamashita, S. Theerasilp, T. Aiuchi, K. Nakaya, Y. Nakamura, Y. Kurihara, Purification and complete amino acid sequence of a new type of sweet protein taste-modifying activity, curculin, J. Biol. Chem. 265 (26) (1990) 15770–15775.
[6] X. Liu, S. Maeda, Z. Hu, T. Aiuchi, K. Nakaya, Y. Kurihara, Purification, complete amino acid sequence and structural characterization of the heat-stable sweet protein, mabinlin II, Eur. J. Biochem. 211 (1–2) (1993) 281–287.
[7] D. Ming, G. Hellekant, Brazzein, a new high-potency thermostable sweet protein from Pentadiplandra brazzeana B, FEBS Lett. 355 (1) (1994) 106–108.
[8] T. Tancredi, A. Pastore, S. Salvadori, V. Esposito, P.A. Temussi, Interaction of sweet proteins with their receptor. A conformational study of peptides corresponding to loops of brazzein, monellin, and thaumatin, Eur. J. Biochem. 271 (11) (2004) 2231–2240.
[9] S. Theerasilp, Y. Kurihara, Complete purification and characterization of the taste-modifying protein, miraculin, from miracle fruit, J. Biol. Chem. 263 (23) (1988) 11536–11539.
[10] H. Igeta, Y. Tamura, K. Nakaya, Y. Nakamura, Y. Kurihara, Determination of disulfide array and subunit structure of taste-modifying protein, miraculin, Biochim. Biophys. Acta 1079 (3) (1991) 303–307.
[11] K. Ito, T. Asakura, Y. Morita, K. Nakajima, A. Koizumi, A. Shimizu-Ibuka, K. Masuda, M. Ishiguro, T. Terada, J. Maruyama, K. Kitamoto, T. Misaka, K. Abe, Microbial production of sensory-active miraculin, Biochem. Biophys. Res. Commun. 360 (2) (2007) 407–411.
[12] P. Jiang, Q. Ji, Z. Liu, L.A. Snyder, L.M. Benard, R.F. Margolskee, M. Max, The cysteine-rich region of T1R3 determines responses to intensely sweet proteins, J. Biol. Chem. 279 (43) (2004) 45068–45075.
[13] P.A. Temussi, Why are sweet proteins sweet? Interaction of brazzein, monellin and thaumatin with the T1R2–T1R3 receptor, FEBS Lett. 526 (1–3) (2002) 1–4.
[14] G. Morini, A. Bassoli, P.A. Temussi, From small sweeteners to sweet proteins: anatomy of the binding sites of the human T1R2–T1R3 receptor, J. Med. Chem. 48 (17) (2005) 5520–5529.
[15] V. Esposito, R. Gallucci, D. Picone, G. Saviano, T. Tancredi, P.A. Temussi, The importance of electrostatic potential in the interaction of sweet proteins with the sweet taste receptor, J. Mol. Biol. 360 (2) (2006) 448–456.
[16] A. Shimizu-Ibuka, Y. Morita, T. Terada, T. Asakura, K. Nakajima, S. Iwata, T. Misaka, H. Sorimachi, S. Arai, K. Abe, Crystal structure of neoculin: insights into its sweetness and taste-modifying activity, J. Mol. Biol. 359 (1) (2006) 148–158.
[17] D.E. Walters, G. Hellekant, Interactions of the sweet protein brazzein with the sweet taste receptor, J. Agric. Food Chem. 54 (26) (2006) 10129–10133.
[18] S.F. Altschul, W. Gish, W. Miller, E. Myers, D.J. Lipman, Best local alignment search tool, J. Mol. Biol. 215 (1990) 403–410.
[19] A.M. Facchiano, P. Stiuso, M.L. Chiusano, M. Caraglia, G. Giuberti, M. Marra, A. Abbruzzese, G. Colonna, Homology modelling of the human eukaryotic initiation factor 5A (eIF-5A), Protein Eng. 14 (11) (2001) 881–890.
[20] S. Costantini, M. Rossi, G. Colonna, A.M. Facchiano, Modelling of HLA-DQ2 and its interaction with gluten peptides to explain molecular recognition in celiac disease, J. Mol. Graph. Model. 23 (5) (2005) 419–431.
[21] S. Costantini, G. Colonna, A.M. Facchiano, Simulation of conformational changes occurring when a protein interacts with its receptor, Comput. Biol. Chem. 31 (3) (2007) 196–206.
[22] A.M. Facchiano, S. Costantini, A. Di Maro, D. Panichi, A. Chambery, A. Parente, S. Di Gennaro, E. Poerio, Modeling the 3D structure of wheat subtilisin/chymotrypsin inhibitor (WSCI). Probing the reactive site with two susceptible proteinases by time-course analysis and molecular dynamics simulations, Biol. Chem. 387 (7) (2006) 931–940.
[23] S. Krauchenco, S.C. Pando, S. Marangoni, I. Polikarpov, Crystal structure of the Kunitz (STI)-type inhibitor from Delonix regia seeds, Biochem. Biophys. Res. Commun. 312 (4) (2003) 1303–1308.
[24] J.D. Thompson, D.G. Higgins, T. Gibson, CLUSTAL W: improving the sensitivity of progressive multiple sequence alignment through sequence weighting, position-specific gap penalties and weight matrix choice, J. Nucleic Acids Res. 22 (1994) 4673–4680.
[25] A. Sali, T.L. Blundell, Comparative protein modelling by satisfaction of spatial restraints, J. Mol. Biol. 234 (1993) 779–815.
[26] R.A. Laskowski, M.W. MacArthur, D.S. Moss, J.M. Thornton, PROCHECK: a program to check the stereochemical quality of protein structures, J. Appl. Cryst. 26 (1993) 283–291.
[27] M.J. Sippl, Recognition of errors in three-dimensional structures of proteins, Proteins 17 (1993) 355–362.
[28] F. Melo, D. Devos, E. Depiereux, E. Feytmans, ANOLEA: a www server to assess protein structures, Proc. Int. Conf. Intell. Syst. Mol. Biol. 5 (1997) 187–190.
[29] S. Tosatto, The Victor/FRST Function for Model Quality Estimation, J. Comput. Biol. 12 (10) (2005) 1316–1327.
[30] Z. Xiang, C.S. Soto, B. Honig, Evaluating conformational free energies: the colony energy and its application to the problem of loop prediction, PNAS 99 (2002) 7432–7437.
[31] J.A. Dalton, R.M. Jackson, An evaluation of automated homology modelling methods at low target template sequence similarity, Bioinformatics 23 (15) (2007) 1901–1908.
[32] W. Kabsch, C. Sander, Dictionary of protein secondary structure: pattern recognition of hydrogen-bonded and geometrical features, Biopolymers 2 (1983) 2577–2637.
[33] C.A. Orengo, A.D. Michie, S. Jones, D.T. Jones, M.B. Swindells, J.M. Thornton, CATH – a hierarchic classification of protein domain structures, Structure 5 (1997) 1093–1108.
[34] J.A. Cuff, G.J. Barton, Application of enhanced multiple sequence alignment profiles to improve protein secondary structure prediction, proteins: structure, Function and Genetics in proteins 40 (2000) 502–511.
[35] B. Rost, C. Sander, R. Schneider, PHD: an automatic mail server for protein secondary structure prediction, Comput. Appl. Biosci. 10 (1) (1994) 53–60.
[36] S.R. Comeau, D.W. Gatchell, S. Vajda, C.J. Camacho, ClusPro: an automated docking and discrimination method for the prediction of protein complexes, Bioinformatics 20 (1) (2004) 45–50.
[37] S.R. Comeau, S. Vajda, J. Carlos, J. Camacho, Performance of the first protein docking server ClusPro in CAPRI Rounds 3–5, Proteins 60 (2005) 239–244.
[38] S. Jones, J.M. Thornton, Principles of protein-protein interactions derived from structural studies, PNAS 93 (1996) 13–20.

[39] S.J. Hubbard, S.F. Campbell, J.M. Thornton, Molecular recognition. Conformational analysis of limited proteolytic sites and serine proteinase protein inhibitors, J. Mol. Biol. 220 (1991) 507–530.
[40] I.K. McDonald, J.M. Thornton, Satisfying hydrogen bonding potential in proteins, J. Mol. Biol. 238 (1994) 777–793.
[41] A. Chambery, M. Pisante, A. Di Maro, E. Di Zazzo, M. Ruvo, S. Costantini, G. Colonna, A. Parente, Invariant Ser211 is involved in the catalysis of PD-L4, type I RIP from Phytolacca dioica leaves, Proteins 67 (1) (2007) 209–218.
[42] C. Gianfrani, R. Siciliano, A.M. Facchiano, A. Camarca, F.M. Mazzeo, S. Costantini, V.M. Savati, F. Maurano, G. Mazzarella, G. Iaquinto, P. Bergamo, M. Rossi, Transamidation of wheat flour inhibits the response to gliadin of intestinal T cells in celiac disease, Gastroenterology 133 (2007) 780–789.
[43] D. Van Der Spoel, E. Lindahl, B. Hess, G. Groenhof, A.E. Mark, H.J. Berendsen, GROMACS: fast, flexible, and free, J. Comput. Chem. 26 (2005) 1701–1718.
[44] L. Esposito, C. Pedone, L. Vitagliano, Molecular dynamics analyses of cross-beta-spine steric zipper models: beta-sheet twisting and aggregation, PNAS 103 (31) (2006) 11533–11538.
[45] W. Humphrey, A. Dalke, K.J. Schulten, VMD: visual molecular dynamics, J. Mol. Graph. 14 (1996) 33–38.
[46] S. Theerasilp, H. Hitotsuya, S. Nakajo, K. Nakaya, Y. Nakamura, Y. Kurihara, Complete amino acid sequence and structure characterization of the taste-modifying protein, miraculin, J. Biol. Chem. 264 (12) (1989) 6655–6659.
[47] N. Takahashi, H. Hitotsuya, H. Hanzawa, Y. Arata, Y. Kurihara, Structural study of asparagine-linked oligosaccharide moiety of taste-modifying protein, miraculin, J. Biol. Chem. 265 (14) (1990) 7793–7798.
[48] P.A. Temussi, Natural sweet macromolecules: how sweet proteins work, Cell Mol. Life Sci. 63 (16) (2006) 1876–1888.
[49] J.R. Hobbs, S.D. Munger, G.L. Conn, Monellin (MNEI) at 1.15 Å resolution, Acta Crystallogr. Sect. F Struct. Biol. Cryst. Commun. 63 (Pt 3) (2007) 162–167.